Bioinformatics, 34, 2018, i245–i253
doi: 10.1093/bioinformatics/bty274
ISMB 2018

OXFORD

DisruPPI: structure-based computational redesign algorithm for protein binding disruption

Yoonjoo Choi[1], Jacob M. Furlon[2], Ryan B. Amos[3], Karl E. Griswold[2,4,5] and Chris Bailey-Kellogg[6,*]

[1]Department of Biological Sciences, Korea Advanced Institute of Science and Technology (KAIST), Daejeon 34141, Republic of Korea, [2]Thayer School of Engineering, Dartmouth, Hanover, NH 03755, USA, [3]Department of Computer Science, Princeton University, Princeton, NJ 08540, USA, [4]Norris Cotton Cancer Center at Dartmouth, Lebanon, NH 03766, USA, [5]Department of Biological Sciences, Dartmouth, Hanover, NH 03755, USA and [6]Department of Computer Science, Dartmouth, Hanover, NH 03755, USA

*To whom correspondence should be addressed.

Abstract

Motivation: Disruption of protein–protein interactions can mitigate antibody recognition of therapeutic proteins, yield monomeric forms of oligomeric proteins, and elucidate signaling mechanisms, among other applications. While designing affinity-enhancing mutations remains generally quite challenging, both statistically and physically based computational methods can precisely identify affinity-reducing mutations. In order to leverage this ability to design variants of a target protein with disrupted interactions, we developed the DisruPPI protein design method (DISRUpting Protein–Protein Interactions) to optimize combinations of mutations simultaneously for both disruption and stability, so that incorporated disruptive mutations do not inadvertently affect the target protein adversely.

Results: Two existing methods for predicting mutational effects on binding, FoldX and INT5, were demonstrated to be quite precise in selecting disruptive mutations from the SKEMPI and AB-Bind databases of experimentally determined changes in binding free energy. DisruPPI was implemented to use an INT5-based disruption score integrated with an AMBER-based stability assessment and was applied to disrupt protein interactions in a set of different targets representing diverse applications. In retrospective evaluation with three different case studies, comparison of DisruPPI-designed variants to published experimental data showed that DisruPPI was able to identify more diverse interaction-disrupting and stability-preserving variants more efficiently and effectively than previous approaches. In prospective application to an interaction between enhanced green fluorescent protein (EGFP) and a nanobody, DisruPPI was used to design five EGFP variants, all of which were shown to have significantly reduced nanobody binding while maintaining function and thermostability. This demonstrates that DisruPPI may be readily utilized for effective removal of known epitopes of therapeutically relevant proteins.

Availability and implementation: DisruPPI is implemented in the EpiSweep package, freely available under an academic use license.

Contact: cbk@cs.dartmouth.edu

Supplementary information: Supplementary data are available at *Bioinformatics* online.

1 Introduction

Due to the importance of protein–protein interactions in myriad cellular processes, much effort has been invested in the development of methods to redesign interacting pairs for desired affinity and specificity, and even to design entirely new partners. Such methods typically focus on improving affinity (Kastritis and Bonvin, 2012), and have driven a wide range of applications (Kortemme and Baker, 2004; Schreiber and Fleishman, 2013), including improvement of antibody binding affinities (Kuroda *et al.*, 2012; Lippow and Tidor, 2007; Lippow *et al.*, 2007), design of inhibitors against infectious

© The Author(s) 2018. Published by Oxford University Press.

This is an Open Access article distributed under the terms of the Creative Commons Attribution Non-Commercial License (http://creativecommons.org/licenses/by-nc/4.0/), which permits non-commercial re-use, distribution, and reproduction in any medium, provided the original work is properly cited. For commercial re-use, please contact journals.permissions@oup.com

organisms (Reynolds *et al.*, 2008; Whitehead *et al.*, 2012), enhancement of T-cell mediated immune recognition (Haidar *et al.*, 2009; Harada *et al.*, 2007; Hawse *et al.*, 2012), epitope-focused vaccine design (Azoitei *et al.*, 2012, 2011) and peptide redesign for cancer detection (Hao *et al.*, 2008).

In some significant applications, the goal is to disrupt binding instead of enhancing it. For example, an existing anti-drug antibody response against a therapeutic protein can be mitigated by mutagenically modifying the positions recognized by the antibody(-ies) (Griswold and Bailey-Kellogg, 2016; Liu *et al.*, 2012; Onda *et al.*, 2008). As another example, monomerization of some oligomeric proteins, such as fluorescent proteins, reduces aberrant aggregation and provides better solubility (Campbell *et al.*, 2002; Nooren and Thornton, 2003). Finally, residues constituting an allosteric hotspot by which one protein passes a signal to another can be identified by testing potentially disruptive mutations (Liu *et al.*, 2013). However, in spite of the importance of these and other applications, little effort has been made regarding general-purpose methods for optimizing binding disruption.

Optimizing the affinity of interacting proteins (for better or worse) requires predicting the effects of mutations on binding. A wide range of approaches to this problem have been pursued, including all-atom molecular dynamics (Deng and Roux, 2009; Moretti *et al.*, 2013; Weis *et al.*, 2006), empirically derived physical potentials (Brender and Zhang, 2015; Guerois *et al.*, 2002; Kortemme and Baker, 2004), statistical contact potentials (Pons *et al.*, 2011; Tharakaraman *et al.*, 2013; Vangone and Bonvin, 2015), machine learning methods combining multiple such features (Dehouck *et al.*, 2013; Wang *et al.*, 2012) and target-specific data-driven models (Kamisetty *et al.*, 2015; Nielsen *et al.*, 2008; Thomas *et al.*, 2009). The curation of extensive databases of experimentally measured binding free energies (Moal and Fernández-Recio, 2012; Sirin *et al.*, 2016) has recently enabled evaluation of the predictive ability of some such methods (i.e. correlation of predicted and experimental $\Delta\Delta G$).

In general, such benchmark studies assess how well scoring functions predict free energy changes over all types of mutations (both enhancing and disrupting binding). However, our focus here is on the selection of mutations that truly are disruptive. This is a somewhat different goal from generally predicting affinity well, or even classifying improved versus weakened binding, as we are willing to miss some disruptive mutations in order to ensure that all the selected mutations are very likely to be disruptive (i.e. accept false negatives in order to eliminate false positives). Intuitively, prediction of binding disruption is easier than binding improvement because only limited free energy space is available for bound states (Goh *et al.*, 2004; Tsai *et al.*, 1999). The recent CAPRI experiment also showed that best performers were particularly good at identifying deleterious (disruptive) mutations of *de novo* hemagglutinin binders (Moretti *et al.*, 2013). Thus we refine previous benchmarks into a binding disruption-focused benchmark and demonstrate that disruption can in fact be predicted quite well by two representative methods: the physically based FoldX (Guerois *et al.*, 2002; Schymkowitz *et al.*, 2005), the best performer in other recent binding benchmarks (Brender and Zhang, 2015; Sirin *et al.*, 2016), and the statistically based INT5 (Pons *et al.*, 2011), part of a scoring function routinely shown to be very successful in protein docking benchmarks (Moal *et al.*, 2013; Pons *et al.*, 2011).

While our new assessment demonstrates the ability of computational methods to specifically identify disruptive mutations, it is also necessary to preserve the stability and function of the protein of interest. It would not be helpful to disrupt a target protein's interactions simply by denaturing it. This requires consideration and optimization of the interrelated effects of sets of mutations on a protein, problems in the field of protein design (Karanicolas and Kuhlman, 2009). In order to simultaneously but independently evaluate and optimize stability and binding disruption, we developed a new method, called DisruPPI (DISRUpting Protein–Protein Interactions). DisruPPI employs a Pareto optimization approach to select mutations making the best trade-offs between these two criteria, designing variants that are predicted to destabilize the protein as little as possible for increasing amounts of binding disruption. This Pareto optimization approach leverages the high performance of binding disruption prediction, sidestepping explicit design of the interface and thus yielding a more focused design problem, while also robustly assessing interrelated effects of mutations on disruption and stability.

We first demonstrate the utility of DisruPPI in three representative retrospective case study applications, where the computational design approach yields more diverse variants than alanine scanning does, while also being more efficient and effective than alanine scanning and other approaches in generating beneficial variants that both disrupt binding and maintain stability and function. We then describe a successful prospective application of DisruPPI to disrupt a previously detailed interaction between enhanced green fluorescent protein (EGFP) and a nanobody (Kubala *et al.*, 2010). This prospective study serves as a model system for deimmunization of therapeutically useful proteins by removing known antigenic sites (antibody epitopes) with minimal sets of mutations.

2 Materials and methods

2.1 Prediction of binding disruption

To predict which mutations may disrupt binding, we consider two computational methods representing quite different approaches: FoldX (Guerois *et al.*, 2002; Schymkowitz *et al.*, 2005) employs an empirical force field, while INT5 (Pons *et al.*, 2011) is a statistical potential derived from amino acid pair propensities at protein–protein interfaces. As is suitable both for these methods in general and for the present application in particular, we seek to disrupt binding with a small number of mutations. With either of these approaches, we represent the predicted mutational effects with a disruption score, for which a positive value indicates that binding is disrupted relative to wild-type.

For FoldX (ver. 4), the wild-type complex structure is repaired and optimized using 'RepairPDB'. Given a mutation or set of mutations, the effect on binding ($\Delta\Delta G$) is then calculated using the 'BuildModel' command; this serves as the disruption score.

For INT5, inter-protein contacting residue pairs are identified in the wild-type complex structure according to a 6 Å distance threshold between non-hydrogen atoms. A sequence-based binding score is then computed as the sum of terms in the INT5 scoring matrix for contacting amino acid pairs, and the disruption score is taken as the difference between the mutant and wild-type binding scores. We note that the INT5 scoring matrix was constructed based on 5 Å threshold (the '5' in the name), but only marginal differences were reported for thresholds ranging from 4 to 6 Å. Thus we chose 6 Å in order to better capture contacts involving larger hydrophobic amino acids such as Trp and Phe (Glaser *et al.*, 2001), whose mutation can be very disruptive.

To assess the performance of the binding disruption predictors, we use two complementary benchmark datasets. AB-Bind was recently curated in order to enable benchmarking of computational

antibody design methods (Sirin *et al.*, 2016). It provides a set of antibody-antigen pairs, each including the wild-type complex structure along with binding affinity data for the wild-type and mutational variants. We note that FoldX was one of the top performers in the AB-Bind evaluation. We selected the 'antibody-antigen'-related mutations from AB-Bind, yielding 20 complexes with a total of 636 mutation sets with associated $\Delta\Delta G$ values. SKEMPI (Moal and Fernández-Recio, 2012) is an even larger database, again with wild-type complex structures and their variant affinity measurements, and including other types of interacting proteins in addition to antibodies and their antigens. To avoid redundancy with AB-Bind, we filtered SKEMPI to non-antibody interactions; for clarity we refer to the reduced database as SKEMPI*. The SKEMPI* database contains 138 interacting protein pairs with a total of 2518 mutation sets and associated affinity values. Variants in the two databases have from 1 to 27 mutations, with >90% of them single or double mutations (Supplementary Fig. S1).

2.1.1 Protein redesign algorithm for binding disruption

The ability to predict whether or not mutations are disruptive is necessary but not sufficient for designing functional, stable, binding-disrupted variants. In order to ensure that the mutations introduced to disrupt binding do not adversely impact the constituent protein(s), we developed DisruPPI to search over possible sets of mutations, designing variants that are predicted to maintain their own stability while having their interaction disrupted. While in general both of the interacting proteins could be redesigned so as to disrupt their interaction, in practice the design is often for just one or the other, so we focus on that case.

DisruPPI designs Pareto optimal variants (Fig. 1), i.e. those making best trade-offs between the predicted impact on binding and the predicted impact on stability, in that no design is better for one aspect without being worse for the other (He *et al.*, 2012; Parker *et al.*, 2010; Thomas *et al.*, 2009). In the example in Figure 1A, Pareto optimal designs were generated for EGFP in order to disrupt the previously characterized binding of a nanobody (Kubala *et al.*, 2010). Figure 1D depicts one example of the optimal designs (top: wild-type and bottom: variant) that are predicted to both maintain EGFP's stability and disrupt nanobody binding. Our experimental results confirm that indeed this particular variant maintains a thermostability on par with wild-type while essentially eliminating nanobody binding.

Full details of the design process are provided in Supplementary Text I. In summary, DisruPPI starts with a set of mutational choices to consider; e.g. those that are evolutionarily accepted or structurally favorable by themselves, and thus most likely to maintain protein stability. It optimizes combinations that are Pareto optimal in terms of a disruption score and a stability score. The current implementation uses INT5 as the disruption score, but could readily incorporate others. Likewise, the implementation is generic to stability score, currently using OSPREY-based assessment of rotameric energies (Chen *et al.*, 2009; Gainza *et al.*, 2012) based on a standard rotamer library (Lovell *et al.*, 2000). Pareto optimal design is done within the general-purpose integer programing framework EpiSweep, previously developed and applied to redesign therapeutic proteins (Choi *et al.*, 2015; Parker *et al.*, 2013). Given a user-specified mutational load, the algorithm 'sweeps' out the Pareto frontier of variants (e.g. circles in Fig. 1A) using that number of mutations to make the best trade-offs between disruption and stability. The process can be iterated to identify near-optimal designs, slightly worse on either or both criteria. It is also run independently over a range of different mutational loads to be considered.

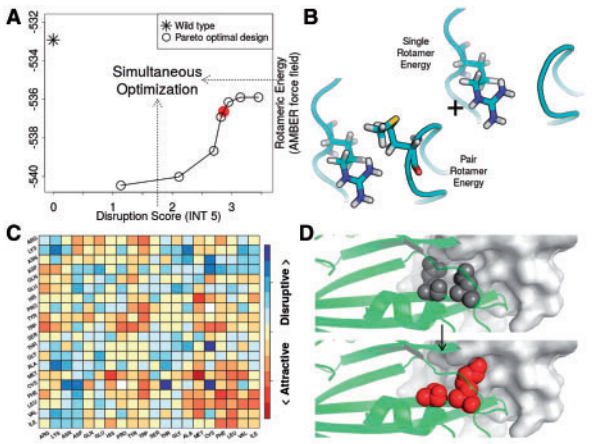

Fig. 1. Overview of DisruPPI DisruPPI generates (**A**) Pareto optimal designs balancing stability and binding by trading off two scores: (**B**) rotameric energy versus (**C**) disruption score. Pareto optimal designs are undominated, in that each design is the best possible for one score without requiring a sacrifice for the other. The designs in (A) are from our prospective application of DisruPPI to a nanobody-EGFP complex. One highly disruptive design (red solid circle) has two mutations, depicted in (**D**, bottom) as R168A (left) and N170K (right) compared to the wild-type (**D**, top). These mutations cause a 105-fold reduction in the binding affinity while maintaining stability and functional fluorescence

2.2 Prospective application to EGFP-nanobody binding

DisruPPI designs were based on an EGFP-nanobody complex structure in the PDB (3OGO, chain B for EGFP and G for the nanobody). Genes including the wild-type EGFP and computationally designed variants, along with the nanobody, were synthesized as gBlocks (IDT) and expressed in *Escherichia coli* BL21 (DE3) followed by HIS-tag purification. Excitation and emission spectra of the expressed variants were measured using SPECTRAmax GEMINI fluorescent plate reader (emission scanning from 475 to 650 nm and excitation scanning from 300 to 530 nm). Emission and excitation maxima were determined by peak fluorescence intensities. Binding affinity was measured by an enzyme-linked immunosorbent assay (ELISA) over different concentrations. Thermostability was measured by differential scanning fluorimetry. Full experimental details are provided in the Supplementary Text II.

3 Results and discussion

3.1 Assessment of protein disruption prediction

This benchmark focuses on identification of mutations that are disruptive. We allow missing some actually disruptive mutations, as long as the ones we identify are highly likely to actually be disruptive, under the assumption that this will give sufficient possibilities for design. Thus our measure is the positive predictive value, $PPV = TP/(TP + FP)$, the ratio between correctly predicted disruptive mutations (TP: true positives) and all mutations predicted to be disruptive (TP plus false positives, FP). Here 'positive' means predicted to be disruptive, i.e. the disruption score exceeds a threshold, which we slide up from 0 to test its impact. 'True' means experimentally determined to be disruptive, for which we use the AB-Bind guideline for medium confidence, $\Delta\Delta G > 0.5$ kcal/mol; 'false' means experimentally determined to be non-disruptive, $\Delta\Delta G \leq 0$ kcal/mol; and

we ignore mutations of uncertain degree of disruptiveness, with $0 < \Delta\Delta G \leq 0.5$ kcal/mol. The AB-Bind dataset includes 350 true, 182 false and 104 ignored, while SKEMPI* has 1363 true, 602 false and 533 ignored.

Both INT5 and FoldX are able to successfully identify disruptive mutations in both benchmarks, achieving consistently high PPV (>0.8) at any disruption score threshold (Supplementary Fig. S2), and trending toward 1 at higher values (i.e. more stringent thresholds yield mostly just disruptive mutations, though fewer of them). Note that both databases are biased, with 66% of AB-Bind mutations truly disruptive along with 69% of SKEMPI* ones, setting baselines for randomly selecting disruptive mutations. Both of the predictors well exceed the random prediction rates, and a combination of the two scores is even better (Supplementary Fig. S3). For example, at a threshold of 0, for the AB-Bind mutations FoldX attains a PPV of 0.83, INT5 0.85 and the combination 0.90; for SKEMPI*, FoldX attains 0.78, INT5 0.81 and the combination 0.85.

While not our focus here, we note that a detailed examination of the scores versus the measurements (Supplementary Fig. S3) reveals that binding improvement is indeed harder to predict, with negative predictive value [TN/(TN + FN)] reaching only 0.61 for FoldX and 0.38 for INT5 (the null is 0.3); where TN is the number of mutations with negative disruption score and $\Delta\Delta G \leq 0$ and FN the number with negative disruption score and $\Delta\Delta G > 0.5$. Thus our focused benchmark reveals the value of separately assessing the ability to select truly disruptive mutations, as opposed to overall accuracy.

3.2 Retrospective case study applications

We applied DisruPPI to redesign three proteins representing different binding disruption applications discussed in the introduction. Other techniques had previously been used to reengineer these proteins for reduced binding. Since the approaches are different, the experimentally tested variants naturally do not include some of the designs that DisruPPI identified, and likewise include some that are not optimal under DisruPPI's metrics. Thus these retrospective tests can only be used to provide an overall qualitative comparison. Nonetheless, we do show that the DisruPPI designs incorporate many of the positions and mutations that had been experimentally determined to be beneficial in terms of disrupting the interaction while still maintaining monomeric structure and function. In contrast to these other approaches, however, the simultaneous optimization approach of DisruPPI enables design for both disruptiveness and stability, instead of separately considering them or relying solely on experiment for one or the other. We demonstrate here that this leads to a more diverse yet better targeted set of variants. Since INT5 and FoldX had comparable performance in our benchmark but INT5 is more computationally efficient than FoldX and still highly predictive, we used it as the disruption predictor in these studies.

3.2.1 Deletion of antibody epitopes in hen egg lysozyme

When an immune response has been established against a therapeutic protein, it may be necessary to mutagenically alter the residues recognized by the matured antibodies ('delete' the antibody epitopes) to reduce detrimental effects and enable effective clinical application (Griswold and Bailey-Kellogg, 2016; Liu *et al.*, 2012; Onda *et al.*, 2008). To evaluate DisruPPI's general ability to design mutations disrupting antibody binding, we targeted the well-studied hen egg lysozyme (HEL) and two anti-HEL antibodies of different binding modes, HyHEL-63 and D1.3. We used binding data from AB-Bind for these antibodies against alanine scanning mutants of HEL (Dall'Acqua *et al.*, 1998; Li *et al.*, 2003).

Mutational choices were collected from homologous sequences to HEL identified by three iterations of PSI-BLAST. The unbound form of HEL (PDB code: 1LSG) was used to compute rotameric energy terms. Contact residues were identified from the complex structures (HyHEL-63: 1DQJ and D1.3: 1VFB). DisruPPI was applied to design variants that disrupt binding of one antibody or the other as well as variants that disrupt them both simultaneously. The effects of mutational load were assessed by considering from one to three mutations per variant. For each mutational load, a curve of all Pareto optimal designs and four near-optimal curves were generated. This yielded a total of 322 designs for HyHEL-63 and 244 for D1.3.

Figure 2A and B depict the Pareto optimal and near-optimal designs at the three mutational loads. We note that, as is typical since the crystal structure was solved to optimize a different score, the wild-type protein is not optimal according to the rotameric energy function and it is possible to find variants with better energies. In general, quite a bit of disruptiveness can be gained before incurring a substantial energetic penalty; this can be calibrated by the disruption score thresholds from the benchmark, where e.g. >90% of the mutations above 0.5 were indeed disruptive in the cases of AB-Bind. As typical, the curves hit an 'elbow' point beyond which additional disruption requires taking less energetically favorable mutations; this naturally tends to come later with higher mutational loads.

The designs include mutations at positions identified by alanine scanning to be disruptive. Seventy two percent of the DisruPPI variants designed to disrupt HyHEL-63 contain mutations at R21 (R21E: 47.5%, R21A: 24.5%). The experimentally tested alanine substitution R21A was found to reduce the binding affinity to be 27.3% of the wild-type. For the DisruPPI designs against D1.3, N19G is the most frequent, but mutating the position may be only marginally disruptive to D1.3 binding; in the experimental results, 74.1% of binding was retained upon alanine substitution. Instead, the second most frequent position, K116, is sufficiently disruptive (49.7% of wild-type binding retained experimentally).

DisruPPI can also be applied to therapeutic proteins where disruption of multiple antibodies is required (Onda *et al.*, 2011). In this case, simultaneous optimization for stability and disruption is critical since multiple mutations (against multiple antibodies) often leads to destabilization of the target protein (Drummond and Wilke, 2009). DisruPPI was applied to design double mutants of HEL in order to disrupt binding of both D1.3 and HyHEL-63. Strikingly, combinations of the mutations that were most frequent in individual antibody designs above (N19 and R21) are predicted to be highly disruptive but energetically worse than the wild-type, and similarly with combined alanine mutations (Fig. 2E). However mutations at R21 and K116 are predicted to be both highly disruptive and energetically favorable. Thus simultaneous design against both antibodies discovered better designs than simply combining independent outcomes. Figure 2F summarizes frequently selected mutations. While R21E is still most frequent, the order of the subsequent frequencies is notably different compared to single antibody designs (Fig. 2C). This further illustrates that the design process is accounting for energetic interactions in maintaining a stable target protein while disrupting its interactions.

In summary, by considering a larger sequence space than just alanine substitutions, and by simultaneously accounting for both

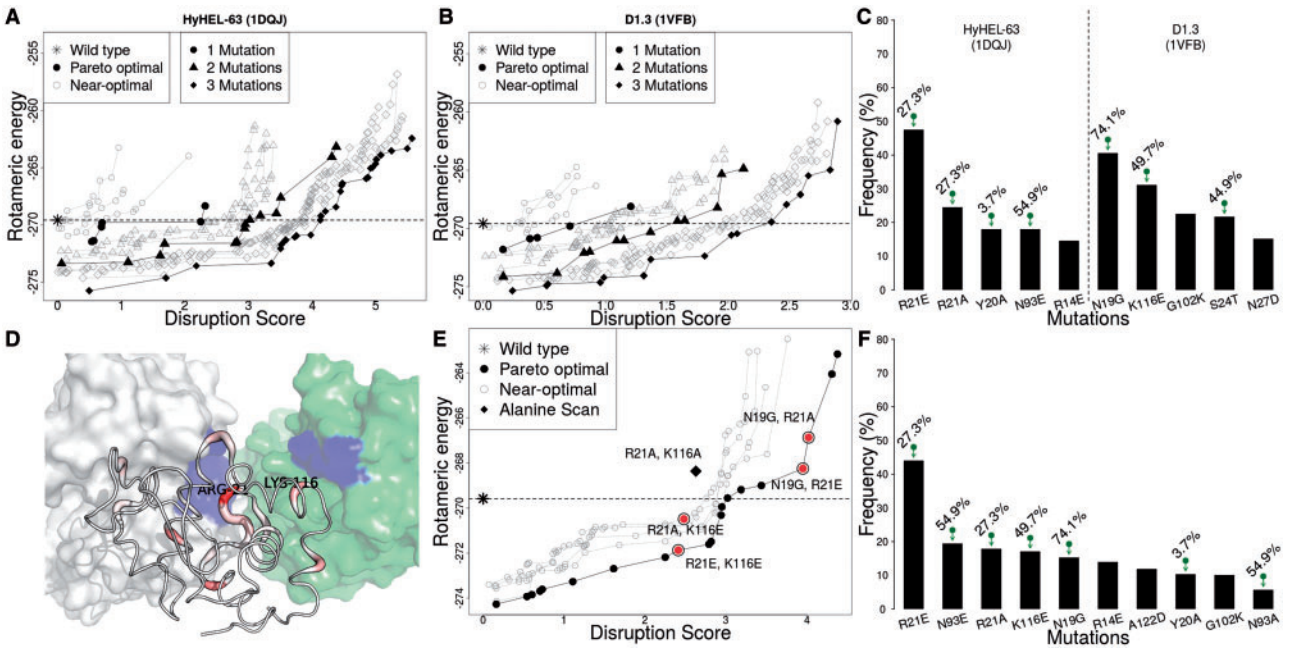

Fig. 2. Design of antibody binding disruption for hen egg lysozyme (HEL) and two antibodies with different binding poses (HyHEL-63 and D1.3). (**A**) and (**B**) Pareto optimal and near-optimal HEL designs independently disrupting each antibody (A: HyHEL-63; B: D1.3) using 1 to 3 mutations. (**C**) Utilization of mutations (bar heights: frequencies across designs) and inferred disruptiveness (numbers above bars: binding affinities of corresponding alanine mutants at those positions, relative to wild-type). (**D**) Visualization of highly disruptive and frequently selected positions for each antibody. HyHEL-63 (PDB code 1DQJ) is rendered as a white surface and D1.3 (1VFB) as a green one. The HEL structure (1LSG) is rendered as a cartoon colored so that the redder, the more frequently targeted. The most frequent positions are labeled (R21 for HyHEL-63 and K116 for D1.3), and contacting antibody residues are colored in blue. (**E**) Pareto optimal and near-optimal curves for double mutants designed to disrupt both antibodies simultaneously. Mutation combinations of top two frequent mutations (R21 for HyHEL-63, N19 and K116 for D1.3) are in solid red circles. (**F**) Mutation frequency and disruptiveness, as in (C), for double mutants disrupting both antibodies.

stability and disruption, DisruPPI can enable more efficient development of more substantially deimmunized variants.

3.2.2 Identification of HIV-1 gp120 allostery-triggering hotspots on CD4

The entry of HIV-1 into a host cell is regulated with large conformational changes in glycoprotein gp120 upon binding of the host cell receptor CD4 (Kwon *et al.*, 2012). Thus identification of binding hotspots on CD4 that trigger the gp120 allosteric restructuring can aid the development of viral entry inhibitors. A recent study identified such hotspots by making alanine substitutions to CD4 along its interface with gp120, and then determining by isothermal titration calorimetry which of the substitutions disrupted binding and thus the associated gp120 allosteric restructuring (Liu *et al.*, 2013).

We applied DisruPPI to likewise select mutations to help identify CD4 binding hotspots. Mutable amino acids were obtained from CD4-related sequences after three iterations of PSI-BLAST. Energies were calculated according to the CD4 structure from its complex with gp120 (PDB code: 1G9N). Since localization of the hotspot position(s) is important, we considered only single point mutations, optimized for both disruption of binding and preservation of stability, focusing just on the optimal designs to keep the comparison focused.

In an alanine scanning study (Liu *et al.*, 2013), 17 positions were tested and 3 (Q25, K35 and F43) were found to yield large free energy changes ($\Delta\Delta G > 0.8$ kcal/mol, Fig. 3A). All three positions were also predicted to be disruptive (red circles in Fig. 3B). DisruPPI identified three Pareto optimal designs, H27N, H27T and F43A. The design predicted to be most disruptive, F43A, was the one that had in fact been experimentally determined to be most disruptive ($\Delta\Delta G = 1.5$ kcal/mol). The mutation also showed large enthalpy change ($\Delta\Delta H = \Delta H(\text{F43A}) - \Delta H(\text{WT}) = -21.4 - (-43.4) = 22$ kcal/mol), i.e. the hotspot position likely caused the allosteric restructuring. The other two Pareto optimal designs at H27 were not experimentally tested. Instead, an alanine substitution at the position (H27A) was tested and found to be not very disruptive but as stable as the wild-type ($\Delta\Delta G < 0.1$ kcal/mol, $\Delta\Delta H > 1$ kcal/mol). This agrees with the model (Fig. 3B), which predicted little disruption and somewhat better energy. It may be speculated that the designed H27N and T would also be marginally disruptive and stable. The other two alanine substitutions (Q25A and K35A) showed medium enthalpy changes ($1 < \Delta\Delta H < 20$ kcal/mol), but it is unclear whether these changes are due to partial allosteric restructuring or instability of CD4. In particular, the lower energy value of K35A versus Q25A could stem from sequentially localized (K35) versus spread out (Q25) interactions with residues in CD4, yielding more wide-ranging impacts of the single mutation at Q25.

In this case study, DisruPPI largely captured experimentally assessed levels of disruption and thermostability. Moreover, one of the three Pareto optimal DisruPPI-designed variants was found to be the binding hotspot that also triggers the allosteric restructuring of gp120. Compared to alanine scanning through all 17 contacting positions, DisruPPI can more efficiently and effectively focus experimental efforts for hotspot identification.

3.2.3 Monomerization of oligomeric red fluorescent protein

Fluorescent proteins (FP) have enabled numerous breakthroughs in the imaging of cellular function and dynamics (Chudakov *et al.*, 2010; Wu *et al.*, 2011). However, most FPs naturally form oligomers, which can in some cases lead to aberrant aggregation hindering

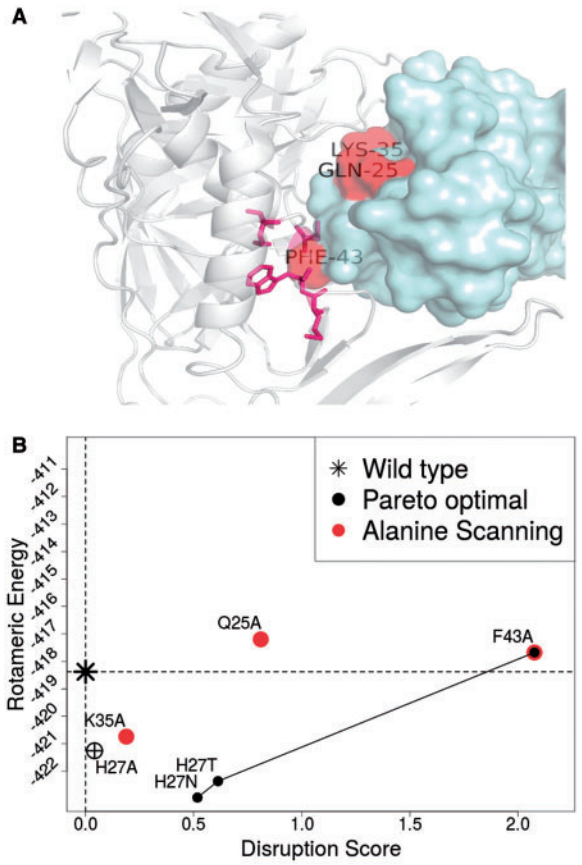

Fig. 3. Identification of CD4 binding hotspots for HIV gp120. (**A**) The complex structure (PDB code 1G9N) of gp120 (cartoon, left) and CD4 (surface, right). An alanine scanning study Liu *et al.* 2013 showed that Q25, K35 and F43 were important for binding. F43A in particular makes tight contacts with hydrophobic amino acids in gp120 (in pink sticks). (**B**) DisruPPI generated three Pareto optimal designs, one of which had been previously tested (F43A) and found to be the most disruptive among a set of 17 alanine mutations in the CD4 interface. The position is involved not only binding but also an allosteric restructuring of gp120. The two other alanine substitutions (Q25A and K35A) are also predicted to be highly disruptive. The two Pareto optimal mutations (H25N and T) may be less disruptive. However the results of H27A, which showed low binding disruption but is as stable as the wild-type, may indicate that the two Pareto optimal mutations are stable as predicted

their production and use (Shemiakina *et al.*, 2012; Wannier *et al.*, 2015). In the case of red FPs (RFPs), all known native RFPs (about 50 to date) are tetrameric and only a few engineered ones are monomeric (Wannier *et al.*, 2015). A recent computationally driven approach demonstrated that resurfacing interface β-strands can aid monomer engineering of *Discosoma* sp. red fluorescent protein (DsRed) (Wannier *et al.*, 2015). The approach created a 'monomeric library' (mLib) targeting 17 interface positions. Ninety-three variants out of 96 in the library were found to be soluble and monomeric.

To enable a direct comparison, we configured DisruPPI with corresponding design settings: target the 17 interface positions for mutation to one of 12 non-hydrophobic amino acids (Ala, Arg, Asn, Asp, Gln, Glu, Gly, His, Lys, Pro, Ser and Thr). A chain of an oligomeric DsRed structure (PDB code: 1ZGO chain A) with the mutations was used to evaluate rotameric energies. Since the mLib variants incorporated from 13 to 16 mutations, we also imposed that mutational load constraint. The 96 mLib designs were selected with the lowest energy values. For direct comparison against the mLib optimized variants, we considered only Pareto optimal designs.

In total, 216 Pareto optimal designs were generated (Fig. 4A). They dominated the mLib variants, in the Pareto sense—for each mLib variant, at least one DisruPPI design was better for both disruption and rotameric energy scores. It is worth noting that the mLib variants exhibit near wild-type energies under the score we used (different from that in the original study), and are also predicted to be disruptive to the oligomer. Thus we would expect the DisruPPI designs to also be stable monomers.

The DisruPPI designs and mLib variants have similar sequence composition, with many amino acids identical or of similar physicochemical properties (Fig. 4B). For instance, in the overlapping disruption score range (<10), T21R is always observed and R216 is always unmutated in both sets, whereas aggressive designs with highly disruptive mutations (>10) and correspondingly higher rotameric energies differ at those positions, perhaps indicating that these are energetically important positions. In fact, the mLib variants are more similar to the aggressive designs (i.e. those with relatively higher rotameric energies) than those with similar disruption scores. Comparing the most frequent mutation at each position, eight positions of the aggressive designs are identical to the mLib variants, while only four are for those in the overlapping disruption score range.

Based on this analysis, we speculated that the rotameric energy and disruption score ranges of the mLib variants could be achieved with a smaller number of mutations. We generated a Pareto optimal set of 5-mutation DisruPPI variants, which were indeed in a similar disruption score range but still with lower rotameric energies (Fig. 4A). A representative 5-mutation plan, Rep5, with disruption score near the representative variant selected for discussion in the previous study (mLib77; 14 mutations) was chosen for a direct comparison. The mutated positions of Rep5 are a subset of mLib77 (Supplementary Table S1). In the structure (Fig. 4C), Rep5 mutations largely overlap the regions covered by mLib77, constituting 65% of the contacting surface area (2530 Å^2 for mLib77 and 1633 Å^2 for Rep5), but requiring only one-third of the mutations.

The results show that DisruPPI is able to generate variants likely to disrupt oligomerization but preserve stable monomers, using a relatively small number of mutations and avoiding extensive experimental effort.

3.3 Prospective disruption of EGFP-nanobody binding interaction

As discussed in Section 1, in the course of therapeutic and vaccine development it may be necessary to eliminate undesired antibody recognition of a protein. To evaluate the utility of disruptive design in this context, we put DisruPPI to prospective use, computationally optimizing and experimentally evaluating variants of EGFP designed to disrupt molecular recognition by a high-affinity nanobody (Kubala *et al.*, 2010) while maintaining molecular function. Complete sets of Pareto optimal designs were generated for mutational loads from 1 to 4 (Supplementary Fig. S4). As discussed for the HEL case study, the most frequently targeted positions over the set of designs may indicate hotspot residues that can be safely mutated to disrupt binding. Figure 5A shows that the top two positions here (R168 and N170, Supplementary Fig. S4B) are at the core of the binding interface between the nanobody and EGFP. In fact, R168 is reported to be a flexible residue involved in binding of known nanobodies (Kirchhofer *et al.*, 2010). Furthermore, all the

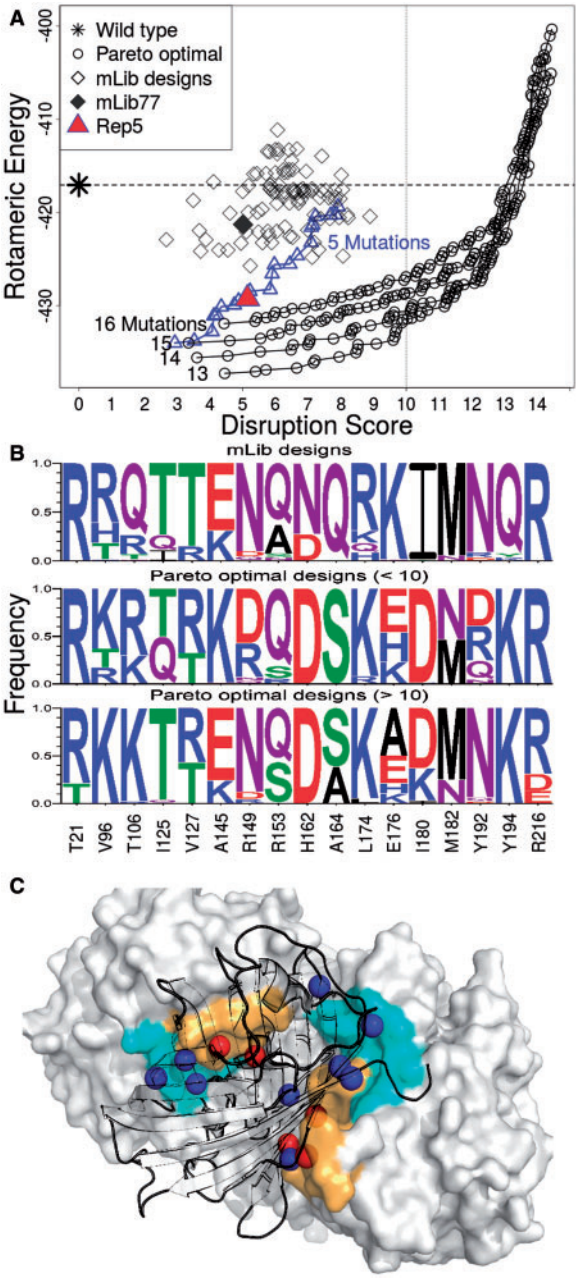

Fig. 4. Monomerization of DsRed. (**A**) DisruPPI designs dominate the 93 mLib variants found to be stable monomers. All the mLib variants including the representative (mLib77) exhibit near wild-type energies and they are also predicted to be disruptive, but the DisruPPI designs are even better. A subsequent set of DisruPPI designs with only five mutations covers the same disruption range as mLib77 but also still with better energies. (**B**) DisruPPI and mLib designs show similar mutation patterns. The mLib variants are in fact closer to aggressive DisruPPI designs (disruption score > 10). (**C**) Variants in the similar disruption and energy ranges of the mLib ones can be achieved by imposing a smaller number of mutations. Rep5 with five mutations (red spheres) largely covers the surface contacting regions (orange surface) of the 14 mutation mLib representative (blue spheres; cyan surface)

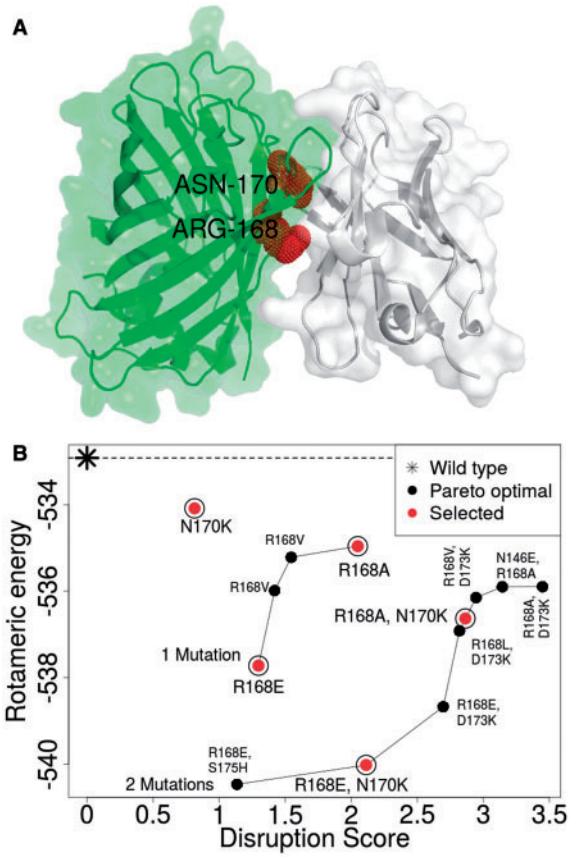

Fig. 5. Design of EGFP variants disruptive to the binding nanobody. (**A**) The two most frequently targeted positions by DisruPPI (R168 and N170) are at the core of the binding interface. The complex structure is 3OGO chain B and G. (**B**) Single and double mutations at the positions are selected for final designs. The single mutation N170K is not a Pareto optimal design but participates in combinations that are

single mutation Pareto optimal designs are at R168 (to A, V, L and E).

We thus computationally evaluated all allowed mutations (individually in combination) at these two positions (Fig. 5). We selected for experimental evaluation the most and least disruptive single mutations at R168 (R168A and R168E) and the only mutational choice at N170 (to K). We augmented these single mutations with their double-mutation combinations (N170K with R168A or R168E).

The engineered variants were produced recombinantly, purified (Supplementary Fig. S5), and assessed for α-GFP nanobody binding, thermostability, and spectral characteristics (Table 1). Binding affinity of the α-GFP nanobody to each EGFP variant was quantified by ELISA, yielding an EC_{50} of 0.44 nM for wild-type EGFP, which was consistent with the previously reported K_d values for this interaction (Kirchhofer *et al.*, 2010; Rothbauer *et al.*, 2006). All five DisruPPI designs exhibited a dramatic reduction in nanobody binding, with EC_{50} values in the range of 1–10 μM, equating to 6000- to 19 000-fold reductions in affinity (Table 1). The predicted disruption scores and rotameric energies of the five EGFP variants fell within relatively narrow ranges, and as a result, there was not a strong correlation with experimental measurements. It bears noting, however, that the double-mutation designs, as predicted, were more disruptive of nanobody binding compared to the single mutation designs and the disruption levels of single mutants tended to be additive. Thus, the disruption score predictions were consistent with overall experimental trends, and we speculate that testing a larger panel of designs covering a wider range of scores might yield better overall correlation with affinity measurements, as we have shown in the context of deimmunization via T-cell epitope deletion (Salvat *et al.*, 2015). While effectively evading nanobody binding, the

Table 1. Experimental characterization of DisruPPI-designed EGFP variants

Variants	Disruption score	Rotameric energy	Nanobody EC_{50} (nM)	Melting temperature (°C)	Excitation Max (nm)	Emission Max (nm)
WT	−0.49	−532.9	0.44 ± 0.01	79	486	511
N170K	0.33	−534.1	2590 ± 60	78	485	512
R168A	1.56	−534.9	3600 ± 200	77	484	512
R168E	0.81	−537.7	5200 ± 300	78	485	510
R168A ± N170K	2.38	−536.6	6800 ± 500	76	484	510
R168E ± N170K	1.63	−540.1	8500 ± 700	78	485	510

DisruPPI variants retained functional fluorescence and high thermostability, exhibiting only 1–3°C reductions in T_m values relative to wild-type EGFP.

4 Conclusion

While methods to predict or enhance protein–protein interactions have been extensively pursued, much less effort has been made toward disrupting protein–protein binding. Here we show that mutations predicted to be disruptive can be confidently used, and we develop a computational redesign program, DisruPPI, leveraging this insight to optimize beneficial sets of such mutations. The algorithm simultaneously optimizes protein stability and disruption, which are otherwise typically treated separately, or not at all. We have demonstrated this method in a diverse set of representative practical cases: antibody–antigen binding disruption, binding hotspot identification and monomerization of oligomeric proteins. DisruPPI proved to be highly effective and efficient compared to previous approaches, finding more diverse variants likely to be disruptive and stable mutations within a smaller pool of candidates for experimental testing. In the case of prospective application to an EGFP-nanobody complex, DisruPPI reduced nanobody binding affinity by four orders of magnitude with only one or two Pareto optimal mutations, while at the same time the engineered variants maintained wild-type thermostability and spectra.

Funding

This work was supported in part by the National Institutes of Health [R01 GM098977 to C.B-K.] and the Korea Research Fellowship Program [2016H1D3A1938246 to Y.C.] through the National Research Foundation of Korea funded by the Ministry of Science, ICT and Future Planning. Computational resources were supported by the National Science Foundation [CNS-1205521 to C.B-K.].

Conflict of Interest: Chris Bailey-Kellogg and Karl E. Griswold are Dartmouth faculty and co-members of the Delaware biotechnology companies Occulo Holdings LLC and Stealth Biologics, LLC. These authors affirm that the data presented in this paper have been reviewed and approved as specified in Chris Bailey-Kellogg's and Karl E. Griswold's Dartmouth conflict of interest management plans. The remaining authors declare no conflict of interest.

References

Azoitei,M.L. *et al.* (2011) Computation-guided backbone grafting of a discontinuous motif onto a protein scaffold. *Science*, **334**, 373–376.

Azoitei,M.L. *et al.* (2012) Computational design of high-affinity epitope scaffolds by backbone grafting of a linear epitope. *J. Mol. Biol.*, **415**, 175–192.

Brender,J.R. and Zhang,Y. (2015) Predicting the effect of mutations on protein-protein binding interactions through structure-based interface profiles. *PLoS Comput. Biol.*, **11**, e1004494.

Campbell,R.E. *et al.* (2002) A monomeric red fluorescent protein. *Proc. Natl. Acad. Sci. USA*, **99**, 7877–7882.

Chen,C.-Y. *et al.* (2009) Computational structure-based redesign of enzyme activity. *Proc. Natl. Acad. Sci. USA*, **106**, 3764–3769.

Choi,Y. *et al.* (2015). Antibody humanization by structure-based computational protein design. *MAbs*, **7**, 1045–1057.

Chudakov,D.M. *et al.* (2010) Fluorescent proteins and their applications in imaging living cells and tissues. *Physiol. Rev.*, **90**, 1103–1163.

Dall'Acqua,W. (1998) A mutational analysis of binding interactions in an antigen- antibody protein- protein complex. *Biochemistry*, **37**, 7981–7991.

Dehouck,Y. *et al.* (2013) BeAtMuSiC: prediction of changes in protein-protein binding affinity on mutations. *Nucleic Acids Res.*, **41**, W333–W339.

Deng,Y. and Roux,B. (2009) Computations of standard binding free energies with molecular dynamics simulations. *J. Phys. Chem. B*, **113**, 2234–2246.

Drummond,D.A. and Wilke,C.O. (2009) The evolutionary consequences of erroneous protein synthesis. *Nat. Rev. Genet.*, **10**, 715–724.

Gainza,P. *et al.* (2012) Protein design using continuous rotamers. *PLoS Comput. Biol.*, **8**, e1002335.

Glaser,F. *et al.* (2001) Residue frequencies and pairing preferences at protein–-protein interfaces. *Proteins*, **43**, 89–102.

Goh,C.-S. *et al.* (2004) Conformational changes associated with protein–protein interactions. *Curr. Opin. Struct. Biol.*, **14**, 104–109.

Griswold,K.E. and Bailey-Kellogg,C. (2016) Design and engineering of deimmunized biotherapeutics. *Curr. Opin. Struct. Biol.*, **39**, 79–88.

Guerois,R. *et al.* (2002) Predicting changes in the stability of proteins and protein complexes: a study of more than 1000 mutations. *J. Mol. Biol.*, **320**, 369–387.

Haidar,J.N. *et al.* (2009) Structure-based design of a t-cell receptor leads to nearly 100-fold improvement in binding affinity for pepmhc. *Proteins*, **74**, 948–960.

Hao,J. *et al.* (2008) Identification and rational redesign of peptide ligands to crip1, a novel biomarker for cancers. *PLoS Comput. Biol.*, **4**, e1000138.

Harada,A. *et al.* (2007) Relationship between the stability of Hen Egg-White lysozymes mutated at sites designed to interact with α-helix dipoles and their secretion amounts in yeast. *Biosci. Biotechnol. Biochem.*, **71**, 2952–2961.

Hawse,W.F. *et al.* (2012) Cutting edge: evidence for a dynamically driven t cell signaling mechanism. *J. Immunol.*, **188**, 5819–5823.

He,L. *et al.* (2012) A divide-and-conquer approach to determine the pareto frontier for optimization of protein engineering experiments. *Proteins*, **80**, 790–806.

Kamisetty,H. *et al.* (2015) Learning sequence determinants of protein: protein interaction specificity with sparse graphical models. *J. Comput. Biol.*, **22**, 474–486.

Karanicolas,J. and Kuhlman,B. (2009) Computational design of affinity and specificity at protein–protein interfaces. *Curr. Opin. Struct. Biol.*, **19**, 458–463.

Kastritis,P.L. and Bonvin,A.M. (2012) On the binding affinity of macromolecular interactions: daring to ask why proteins interact. *J. R. Soc. Interface*, **10**, 20120835.

Kirchhofer,A. *et al.* (2010) Modulation of protein properties in living cells using nanobodies. *Nat. Struct. Mol. Biol.*, **17**, 133–138.

Kortemme,T. and Baker,D. (2004) Computational design of protein–protein interactions. *Curr. Opin. Chem. Biol.*, **8**, 91–97.

Kubala,M.H. *et al.* (2010) Structural and thermodynamic analysis of the Gfp: Gfp–nanobody complex. *Protein Sci.*, **19**, 2389–2401.

Kuroda,D. *et al.* (2012) Computer-aided antibody design. *Protein Eng. Des. Sel.*, **25**, 507–522.

Kwon,Y.D. *et al.* (2012) Unliganded HIV-1 gp120 core structures assume the cd4-bound conformation with regulation by quaternary interactions and variable loops. *Proc. Natl. Acad. Sci. USA*, **109**, 5663–5668.

Li,Y. *et al.* (2003) Dissection of binding interactions in the complex between the anti-lysozyme antibody hyhel-63 and its antigen. *Biochemistry*, **42**, 11–22.

Lippow,S.M. and Tidor,B. (2007) Progress in computational protein design. *Curr. Opin. Biotechnol.*, **18**, 305–311.

Lippow,S.M. *et al.* (2007) Computational design of antibody-affinity improvement beyond in vivo maturation. *Nat. Biotechnol.*, **25**, 1171–1176.

Liu,W. *et al.* (2012) Recombinant immunotoxin engineered for low immunogenicity and antigenicity by identifying and silencing human b-cell epitopes. *Proc. Natl. Acad. Sci. USA*, **109**, 11782–11787.

Liu,Y. *et al.* (2013) Optimization of cd4/gp120 inhibitors by thermodynamic-guided alanine-scanning mutagenesis. *Chem. Biol. Drug Des.*, **81**, 72–78.

Lovell,S.C. *et al.* (2000) The penultimate rotamer library. *Proteins*, **40**, 389–408.

Moal,I.H. and Fernández-Recio,J. (2012) SKEMPI: a structural kinetic and energetic database of mutant protein interactions and its use in empirical models. *Bioinformatics*, **28**, 2600–2607.

Moal,I.H. *et al.* (2013) The scoring of poses in protein-protein docking: current capabilities and future directions. *BMC Bioinformatics*, **14**, 286.

Moretti,R. *et al.* (2013) Community-wide evaluation of methods for predicting the effect of mutations on protein–protein interactions. *Proteins*, **81**, 1980–1987.

Nielsen,M. *et al.* (2008) Quantitative predictions of peptide binding to any HLA-DR molecule of known sequence: Netmhciipan. *PLoS Comput. Biol.*, **4**, e1000107.

Nooren,I.M. and Thornton,J.M. (2003) Structural characterisation and functional significance of transient protein–protein interactions. *J. Mol. Biol.*, **325**, 991–1018.

Onda,M. *et al.* (2008) An immunotoxin with greatly reduced immunogenicity by identification and removal of b cell epitopes. *Proc. Natl. Acad. Sci. USA*, **105**, 11311–11316.

Onda,M. *et al.* (2011) Recombinant immunotoxin against b-cell malignancies with no immunogenicity in mice by removal of b-cell epitopes. *Proc. Natl. Acad. Sci. USA*, **108**, 5742–5747.

Parker,A.S. *et al.* (2010) Optimization algorithms for functional deimmunization of therapeutic proteins. *BMC Bioinformatics*, **11**, 180.

Parker,A.S. *et al.* (2013) Structure-guided deimmunization of therapeutic proteins. *J. Comput. Biol.*, **20**, 152–165.

Pons,C. *et al.* (2011) Scoring by intermolecular pairwise propensities of exposed residues (sipper): a new efficient potential for protein–protein docking. *J. Chem. Inf. Model.*, **51**, 370–377.

Reynolds,K.A. *et al.* (2008) Computational redesign of the SHV-1 β-lactamase/β-lactamase inhibitor protein interface. *J. Mol. Biol.*, **382**, 1265–1275.

Rothbauer,U. *et al.* (2006) Targeting and tracing antigens in live cells with fluorescent nanobodies. *Nat. Methods*, **3**, 887–889.

Salvat,R.S. *et al.* (2015) Protein deimmunization via structure–based design enables efficient epitope deletion at high mutational loads. *Biotechnol. Bioeng.*, **112**, 1306–1318.

Schreiber,G. and Fleishman,S.J. (2013) Computational design of protein–protein interactions. *Curr. Opin. Struct. Biol.*, **23**, 903–910.

Schymkowitz,J. *et al.* (2005) The foldx web server: an online force field. *Nucleic Acids Res.*, **33**, W382–W388.

Shemiakina,I. *et al.* (2012) A monomeric red fluorescent protein with low cytotoxicity. *Nat. Commun.*, **3**, 1204.

Sirin,S. *et al.* (2016) Ab-bind: antibody binding mutational database for computational affinity predictions. *Protein Sci.*, **25**, 393–409.

Tharakaraman,K. *et al.* (2013) Redesign of a cross-reactive antibody to dengue virus with broad-spectrum activity and increased in vivo potency. *Proc. Natl. Acad. Sci. USA*, **110**, E1555–E1564.

Thomas,J. *et al.* (2009) Graphical models of protein–protein interaction specificity from correlated mutations and interaction data. *Proteins*, **76**, 911–929.

Tsai,C.-J. *et al.* (1999) Folding funnels, binding funnels, and protein function. *Protein Sci.*, **8**, 1181–1190.

Vangone,A. and Bonvin,A.M. (2015) Contacts-based prediction of binding affinity in protein–protein complexes. *Elife*, **4**, e07454.

Wang,L. *et al.* (2012) Prediction of hot spots in protein interfaces using a random forest model with hybrid features. *Protein Eng. Des. Sel.*, **25**, 119–126.

Wannier,T.M. *et al.* (2015) Computational design of the β-sheet surface of a red fluorescent protein allows control of protein oligomerization. *PLoS One*, **10**, e0130582.

Weis,A. *et al.* (2006) Ligand affinities predicted with the MM/PBSA method: dependence on the simulation method and the force field. *J. Med. Chem.*, **49**, 6596–6606.

Whitehead,T.A. *et al.* (2012) Optimization of affinity, specificity and function of designed influenza inhibitors using deep sequencing. *Nat. Biotechnol.*, **30**, 543–548.

Wu,B. *et al.* (2011) Modern fluorescent proteins and imaging technologies to study gene expression, nuclear localization, and dynamics. *Curr. Opin. Cell Biol.*, **23**, 310–317.